Available online at www.sciencedirect.com
ScienceDirect
Biomaterials 28 (2007) 2572–2581
Biomaterials
www.elsevier.com/locate/biomaterials

Nanotoxicity of iron oxide nanoparticle internalization in growing neurons

Thomas R. Pisanic II[a,*], Jennifer D. Blackwell[a], Veronica I. Shubayev[b,d], Rita R. Fiñones[c], Sungho Jin[c]

[a]Department of Bioengineering, University of California, San Diego La Jolla, CA 92093, USA
[b]Department of Anesthesiology, University of California, San Diego School of Medicine La Jolla, CA 92093, USA
[c]Mechanical and Aerospace Engineering Department, University of California, San Diego La Jolla, CA 92093, USA
[d]San Diego Veteran Affairs Medical Healthcare System, La Jolla, CA 92093, USA

Received 29 October 2006; accepted 31 January 2007
Available online 11 February 2007

Abstract

Magnetic nanoparticles (MNPs) have shown great promise for use as tools in a wide variety of biomedical applications, some of which require the delivery of large numbers of MNPs onto or into the cells of interest. Here we develop a quantifiable model cell system and show that intracellular delivery of even moderate levels of iron oxide (Fe_2O_3) nanoparticles may adversely affect cell function. More specifically, we show that exposure to increasing concentrations of anionic MNPs, from 0.15 to 15 mM of iron, results in a dose-dependent diminishing viability and capacity of PC12 cells to extend neurites in response to their putative biological cue, i.e. nerve growth factor. The cytotoxicity results of biomaterials in our model system imply that more study into the acute and long-term effects of cellular Fe_2O_3 internalization is both warranted and necessary.

Keywords: Nanoparticle; Magnetism; Neural cell; Cytotoxicity; Biocompatibility

1. Introduction

The delivery of magnetic nanoparticles (MNPs) to or into various cell types has become an area of increasing interest in the biomedical sciences [1,2]. For example, cell labeling with MNPs is now a widely used means of *in vitro* cell separation, where a high gradient magnetic field is used to isolate cells of interest, tagged with magnetic particles via phenotypic markers, from a heterogeneous population [3,4]. Targeted delivery is used to deliver drugs or genes regio-specifically by attaching them to MNPs and locally concentrating the resulting complexes *in vivo* to the desired locale [5,6]. Similarly, magnetic hyperthermia, the local concentration of MNPs and subsequent heating via AC magnetic fields, has shown promise as a potentially viable cancer therapy [7,8]. And it has additionally been shown that if cells are labeled with large enough numbers of MNPs, that these cells can be located, tracked and recovered using imaging techniques such as high-resolution magnetic resonance imaging (MRI) [9,10]. While these imaging technologies boast exceeding sensitivities, cells of interest must be labeled with relatively large amounts of magnetic material in order to be readily detected. Due to this constraint, much effort has been dedicated to the development of efficient mechanisms of delivery of MNPs into cells of interest.

Many groups have investigated the use of various organic coatings as a means of optimizing the delivery of MNPs to or into cells. Toward these ends, MNPs have been coated with ligands to cell surface receptors [11,12] in order to utilize a receptor-mediated endocytotic pathway, amphiphilic coatings such as polyethylene glycol (PEG) [13,14] or dendrimers [15] to allow their free passage into cells and also with well-known transfection agents such as the HIV-derived TAT protein [9,10]. In several cases it has

*Corresponding author. Magnesensors, Inc., 9717-A Pacific Heights Blvd., San Diego, CA 92121, USA. Tel.: +1 858 4585748; fax: +1 858 452 8733.
E-mail address: tomp@magnes.com (T.R. Pisanic II).

0142-9612/$ - see front matter © 2007 Elsevier Ltd. All rights reserved.
doi:10.1016/j.biomaterials.2007.01.043

been shown that even a simple dimercaptosuccinic acid (DMSA) coating can improve uptake efficiency by three orders of magnitude, presumably by engendering the MNPs with an anionic charge, resulting in nonspecific adsorption to the cell surface followed by endocytosis into the cell [16–18]. Indeed these techniques succeed in delivering large numbers of MNPs into the cells (up to 3–4 orders of magnitude over fluid phase endocytosis), but a valid concern arises over the effects that large intracellular concentrations of iron oxide (Fe_2O_3) might have on normal cell behavior.

In addition to magnetic tracking, many biomedical applications of MNPs such as targeted drug delivery and hyperthermia require very large amounts of MNPs to be injected or targeted to the cells or area of interest. While historically Fe_2O_3 nanoparticles are considered to be well tolerated *in vivo* [19,20], the effects of moderate to high intracellular concentrations of Fe_2O_3 nanostructures upon cell function remain to be adequately elucidated. Although a few studies have been performed investigating the acute cytotoxicity of MNPs and their qualitative effects upon cellular morphology [13,20–24], little work has focused on quantifying the effects that Fe_2O_3 internalization has upon cell behavior and, in particular, the ability of cells to appropriately respond to biological cues. For example, Curtis et al. studied the effects that various nanoparticle surface coatings had on cellular morphology, uptake efficiency, cytotoxicity and, in one case, cell mobility [13,21,22]. Indeed, these papers have shown that nanoparticles and the surface coatings employed can have a dramatic effect upon the *relative* cell behavior and morphology. More quantitatively, Hussain et al. [25] presented data on the effects that various metal/metal oxide nanomaterials had upon liver cell function *in vitro*. Here we demonstrate with an established biomedically used Fe_2O_3 nanoparticle and surface coating preparation, viz. anionic MNPs (AMNPs), that changes in cell behavior and phenotype can be quantified and directly correlated with the level of AMNP exposure.

Enhanced endocytosis via [anionic] DMSA coating is a simple, efficient and well-characterized method of intracellular delivery of Fe_2O_3 nanoparticles. While several studies have clearly shown little to no *in vivo* toxicity of either of these components individually [19,20,26], only recently have they been combined to deliver large numbers of nanoparticles into cells [16–18,27]. In order to clearly evaluate the effects that Fe_2O_3 nanoparticle internalization might have upon cell behavior, phenotype and response to biological cues, a readily quantifiable model cell system was chosen. The PC12 pheochromocytoma clonal cell line has served as a paradigm for neurobiological and neurochemical studies [28]. A prominent characteristic of PC12 cells is their readily quantifiable, rapid and reversible response to nerve growth factor (NGF), resulting in the extension of neurite-like processes up to 1 cm in length, comparable to those of sympathetic neurons [29]. Here we examine and quantify the specific effects that DMSA-coated MNPs have upon cultured PC12 cells and evaluate their ability to respond to NGF as compared to control cells. The focus of this paper is thus on the cytotoxicological evaluation of a previously characterized nanostructure intended and accepted for biomedical uses and its effect upon a readily quantifiable model cell system.

2. Materials and methods

2.1. AMNP synthesis

Maghemite nanoparticles were synthesized as previously described in [30]. Two starting solutions were made by adding 5.406 g of $FeCl_3$ (Sigma-Aldrich, St. Louis, MO) to 20 ml of deionized (DI) water and, separately, adding 1.988 g of $FeCl_2$ (Sigma-Aldrich) to 5 ml of a 2 N solution of HCl (Sigma-Aldrich). These solutions were then added to 100 ml of DI water under vigorous stirring, to which 120 ml of a 2 M ammonia solution was added and remained under vigorous stirring for 5 min, during which, a black precipitate formed, indicating the synthesis of Fe_3O_4. This solution was centrifuged at 900*g* for 5 min, the supernatant was removed and the nanoparticle solution was redispersed in DI water. This solution was centrifuged at 900*g* for 5 min and resuspended in DI water. This washing process was repeated 4 additional times and the centrifugate was finally resuspended in 35 ml of DI water, resulting in an opaque black solution. This solution was heated to 80 °C and the MNPs were oxidized, by bubbling oxygen for 2 h, to Fe_2O_3, as indicated by a dark brown color. The mass of resulting maghemite was determined through drying and weighing to be 1.68 g of Fe_2O_3 in 50 ml of DI water.

DMSA coating was performed as previously described [31]. Separately, 0.26 g of DMSA (Sigma-Aldrich) was added to 313 ml of deoxygenated DI water (via 1 h of nitrogen bubbling) and 205 ml of deoxygenated DI water was added to the maghemite solution. These solutions were deoxygenated for an additional 2 h at room temperature. The maghemite solution was then vigorously stirred while bubbling nitrogen and the pH of both solutions was adjusted to 3.0 with HNO_3 prior to mixing the solutions under vigorous stirring with constant nitrogen bubbling. The reaction was allowed to proceed for 30 min and the resulting mixture was spun down at 800 g for 5 min and resuspended in 200 ml of DI water. Under constant stirring, the pH of this solution was adjusted with NaOH to 9.25–9.5 and maintained for 30 min before lowering the pH to 7.4 with HCl. The resulting solution was centrifuged at 1000*g* for 10 min to remove any precipitated aggregates and the resulting opaque dark brown supernatant was deoxygenated, sterile filtered and stored under nitrogen at 4 °C. The final stock concentration of Fe_2O_3 was adjusted with DI water to 150 mM Fe concentration.

2.2. PC12 cell culture

The rat pheochromocytoma cell line PC12M was derived from the PC12 line by Marc Montminny (Salk Institute, La Jolla, CA) and exhibits increased adherence to polystyrene dishes. The line was grown in high-glucose Dulbecco's modified Eagles medium (DMEM) (Gibco, Grand Island, NY) containing 10% fetal bovine serum (FBS) (Invitrogen, Carlsbad, CA), 5% heat-inactivated horse serum (Omega Scientific Inc.), 100 U/ml penicillin and 100 mg/ml streptomycin (Gibco) at 37 °C in 5% CO_2 until reaching 70% confluence.

2.3. Delivery of AMNPs into PC12 cells

PC12 cells were plated from culture at a concentration of approximately 20,000 cells/ml into 6 or 12 well plates, at volumes of 2 and 1 ml, respectively, in high-glucose DMEM (Gibco) containing 10% FBS (Invitrogen), 5% heat-inactivated horse serum (Omega Scientific Inc.), 100 U/ml penicillin and 100 mg/ml streptomycin (Gibco) at 37 °C and allowed to adhere for 2 days. The following day, the cells were washed and

the media was replaced with serum and phosphate-free HEPES-buffered DMEM (Invitrogen) in order to prevent particle agglomeration. To this solution a concentrated stock solution of AMNPs ([Fe] = 150 mM) was added, yielding final iron concentrations of 15, 1.5 mM and 150 μM, as well as a phosphate-free HEPES-buffered DMEM only control. After overnight incubation, the cells were washed and the modified DMEM was replaced with media containing 1% FBS, 5% heat-inactivated horse serum and 1% penicillin-streptomycin; NGF (Sigma-Aldrich) was added to a working concentration of 100 ng/ml to induce sprouting. The cells were cultured with this media, including changes every other day, for the remainder of each experiment.

2.4. Transmission electron microscopy

For AMNP only analyses, the samples were dried onto a carbon TEM grid and were observed using a transmission electron microscope (TEM) (FEI Sphera Tecnai T^2). For cell samples, cells were plated as described above into 6 well size Petri dishes. Twenty-four hours following exposure to AMNPs, cells were fixed in an aqueous solution of 100 mM sodium cacodylate (Sigma-Aldrich) containing 2% paraformaldehyde (Sigma-Aldrich) and 2% glutaraldehyde (Sigma-Aldrich) at 37 °C for 2 min and then allowed to cool to room temperature for 25 min. The cells were then washed 3 times in ice-cold 100 mM cacodylate buffer and kept on ice. Cells were then post-fixed in ice cold 100 mM sodium cacodylate containing 1% osmium tetroxide (Sigma-Aldrich) for 30 min on ice and then washed 3 times with ice cold DI water followed by a 30 min post fixation in 2% uranyl acetate (Fluka, Seelze, Switzerland) and another three washes with ice cold DI water. The samples were then serially dehydrated in ethanol at room temperature and finally embedded in Durcupan (Fluka), which was sectioned prior to TEM analysis. The samples were then placed onto a carbon TEM grid and were observed using a TEM (JEOL 200CX).

2.5. Live/dead cell staining and cell detachment quantification

Cells were plated as described above in 12 well plates. Prior to, 2, 4 and 6 days following AMNP exposure, the cells were first washed in PBS at 37 °C and left in 1 ml of PBS/well. Calcein AM and ethidium homodimer-1 (ethyl-D) were used from a LIVE/DEAD Viability/Cytotoxicity Kit (Invitrogen) and diluted with PBS to a final concentration of 10 μM each. Each well was aspirated and 20 μl of both stain solutions was added to each well and incubated at 37 °C for 20 min. The samples were analyzed via fluorescent microscopy with appropriate fluorescent filter cubes (FITC cube for calcein, TRITC cube for ethyl-D). A total of at least 300 cells were counted per condition per sample per timepoint, with green fluorescence (emission 515 nm) indicating living cells and red fluorescence (emission 635 nm) indicating dead cells. Cell detachment was quantified by taking media samples from the culture wells 2, 4 and 6 days following AMNP exposure and determining the cell density, and thus total detached cells/well, using a standard hemocytometer (Hausser Scientific, Horsham, PA).

2.6. Fluorescent microscopy

The PC12 cells were plated as described above into 6 well plates containing sterile glass coverslips; 2 , 4 and 6 days following AMNP exposure the coverslips from particular wells of each exposure condition were removed and extracted in a solution of 10 mM 2-morpholinoethanesulfonic acid (MES) buffer (Sigma-Aldrich), 138 mM KCl, 3 mM $MgCl_2$, 2 mM EDTA and 320 mM sucrose for 45 s, followed by fixation in the same buffer containing 4% formaldehyde for 15 min. The coverslips were then washed once in Tris buffered saline (TBS) (150 mM NaCl, 20 mM Tris-HCl, pH 7.4) and stored in TBS at 4 °C until staining. At the time of staining, the samples were permeabilized in a solution of TBS containing 0.5% Triton-X 100 (TX) for 10 min and then rinsed 3 times in TBS containing 0.1% TX for 4 min each rinse. The samples were then blocked in a solution of TBS-0.1% TX with 2% BSA (Sigma-Aldrich), and 0.1% sodium azide (Sigma-Aldrich) for 10 min, followed by incubation for 20 min with mouse anti-tubulin (Molecular Probes, Eugene, OR) diluted to 1 μg/ml in the blocking buffer. The samples were then washed four times in TBS-0.1% TX and fluorescein conjugated anti-mouse secondary antibody was then added at 5 μg/ml of blocking buffer and incubated for 20 min. The samples were washed 4 times in TBS-0.1% TX and then incubated with rhodamine-phalloidin diluted in blocking buffer to 1 μg/ml for 20 min and then washed twice in TBS-0.1% TX. Finally the samples were rinsed once in TBS, once in DI water, drained and mounted onto glass slides. The samples were then analyzed by standard fluorescent microscopy (DMIRB microscope; Leica, Wetzlar, Germany) at 100× with fluorescein and rhodamine filter cubes (Leica), for microtubules and actin, respectively.

2.7. Neurite morphometry

Six days following exposure to AMNPs, the 6 well plate samples were analyzed via phase contrast microscopy at a magnification of 10×. Micrographs of random areas of the culture plates were taken and subsequently analyzed with ImageJ (NIH, Bethesda, MD) for number of neurites per cell, length per neurite and number of intercellular processes per cell. Depending on the growth characteristics, 30–50 cells were analyzed for each parameter for each experimental condition.

2.8. Western blot

Six days following exposure to AMNPs, cells were lysed in a 50 mM Tris-HCl buffer containing 10% glycerol, 0.1% sodium dodecyl sulfate (SDS) (Sigma-Aldrich), 1% TX, 150 mM NaCl, 1.5 mM $MgCl_2$, and protease inhibitors [2 μg/ml aprotinin, 50 μM leupeptin, 1 μM pepstatin, 10 mM phenylmethylsulfonyl fluoride (PMSF) and 5 mM EDTA]. The samples were then reduced in 10% β-mercaptoethanol and centrifuged at 13,000 RPM for 5 min. Thirty μg of protein was added to each lane of 10% SDS-polyacrylamide gel and underwent electrophoresis at 160 V for 90 min. The separated protein was then transferred to a nitrocellulose membrane at 50 V for 1 h in a Tris-glycine transfer buffer (Invitrogen) containing 12 mM Tris base, 95 mM glycine, and 20% methanol. The membranes were then blocked in 5% nonfat dry milk (Bio-Rad, Hercules, CA) for 1 h and incubated overnight at 4 °C with anti-GAP-43 (Sigma-Aldrich) antibody diluted 1:1000 in a 1% BSA solution. Horseradish peroxidase conjugated goat anti-mouse IgG (ECL Kit; Amersham, Arlington Heights, IL) was then applied for 1 h at room temperature. The blots were developed in luminol and exposed to Hyperfilm ECL (Amersham). The blots were stripped and normalized by reprobing with a gel loading (β-actin) control. The molecular weights were compared with prestained low-range standards (Bio-Rad).

3. Results

The final AMNP product was a highly concentrated aqueous ferrofluid, stable over a wide range of pH and salt concentrations. Fig. 1A shows a TEM image of the dried final ferrofluid with average nanoparticle diameters between 5 and 12 nm. The observation of apparent aggregation in Fig. 1A is an artifact of the drying process for standard TEM sample preparation, as the AMNP fluid itself is *highly* stable against aggregation in water and many other aqueous-based buffer solutions. As previously stated, AMNPs have been shown to be readily taken up by a variety of cells via an endocytotic mechanism. The internalization of AMNPs by PC12 cells was verified using TEM. Fig. 1B shows large numbers of AMNPs free within the cytoplasm and contained inside numerous endosomes, accumulated in the perinuclear region within the cells.

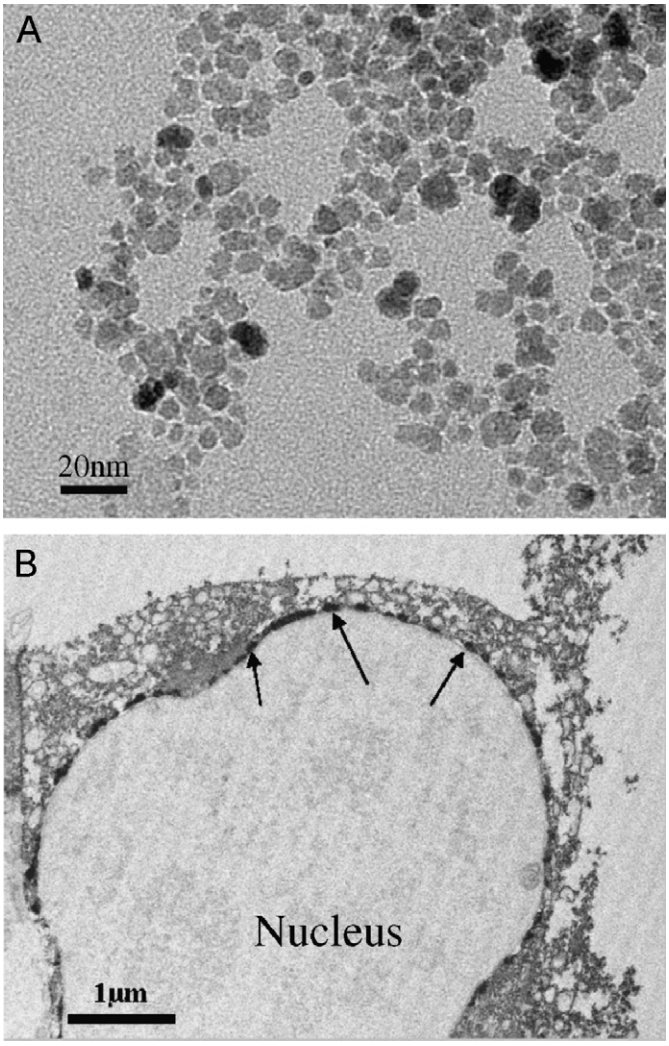

Fig. 1. Transmission electron micrographs of (A) dried anionic Fe_2O_3 magnetic nanoparticles (note that the apparent aggregation is an artifact of sample preparation) and (B) PC12 cell following 24 h exposure to AMNP at Fe concentration of 1.5 mM; arrows indicate typical endosomes containing the magnetic nanoparticles.

It was additionally noted that the intracellular levels of AMNPs were qualitatively proportionate to the added concentrations of the particles (data not shown).

3.1. Acute cytotoxicity

In the initial assessment into the effects of AMNP internalization, standard cytotoxicological evaluations of acute toxicity to the cells were performed using a fluorescent live/dead stain. The stain consists of the dyes calcein AM and ethylidium homodimer-1 (EthD-1), which stain for live and dead cells, respectively. Live cells are stained by membrane-permeant non-fluorescent calcein AM which is converted by intracellular esterases of live cells to the brightly fluorescent calcein, yielding a uniform green fluorescence inside the cells. EthD-1 is non-permeant and is extruded by the intact membrane of live cells; in compromised membranes of dead cells, however, EthD-1 directly binds to nucleic acids and undergoes a 40-fold increase in red fluorescence. Fluorescent images of cells stained with the live (green) and dead (red) stain 6 days after AMNP exposure are shown in Figs. 2A (15 mM iron concentration) and 2B (Control cells). Assessment of cell viability ($n = 300$ per timepoint) through a series of experiments demonstrates statistically significant reductions in PC12 cell viability after exposure to the particles (Fig. 2C). Almost all observed cell death occurs within the first 48 h following incubation with the particles and the total observed cell death increases as a function of AMNP exposure concentration. In addition to cell death, significant cell detachment was also hemocytometrically quantified from the media and observed to correlate to AMNP exposure. A plot of total cell detachment per well as a function of time post exposure to various AMNP concentrations is shown in Fig. 2D.

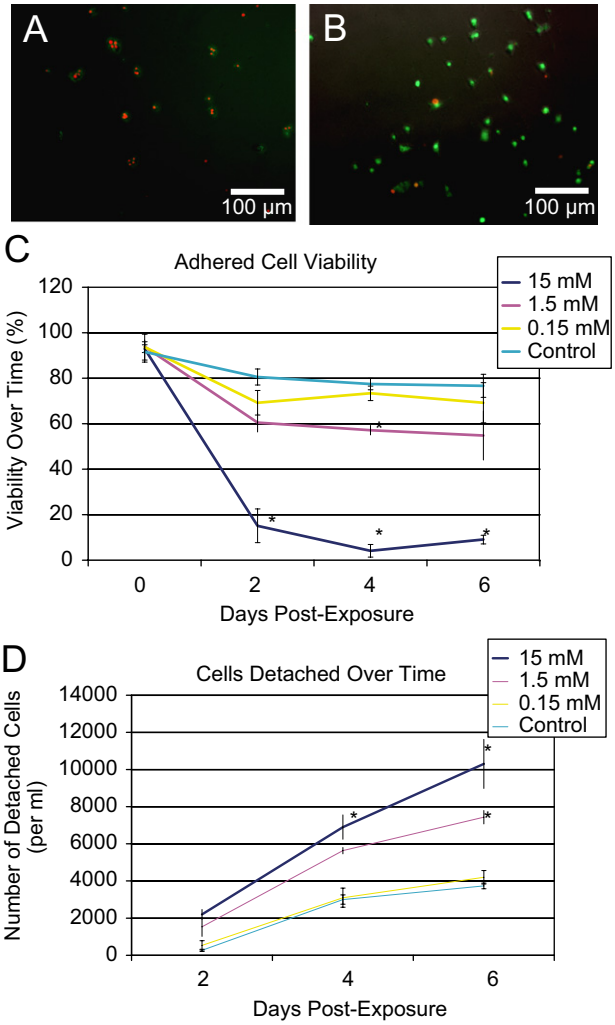

Fig. 2. Live (green)/dead (red) stain of NGF induced PC12 cells 4 days after AMNP exposure at Fe concentration of 15 mM (A) and 0 mM (B, control). Note reduced cell viability (C) and attachment (D) after AMNP exposure at different Fe concentrations. (*Statistics*: one-way ANOVA with Tukey's *post-hoc*, expressed as mean ± standard error, $*p < 0.05$, $**p < 0.01$.)

3.2. Alterations in cytoskeletal structure

In addition to PC12 cell viability, their phenotype and ability to respond to NGF were also affected by increasing concentrations of AMNPs. These differences can be readily observed and qualitatively analyzed optically through phase contrast and immunofluorescent microscopy. Typical PC12 cells, prior to NGF exposure, are undifferentiated, spherical in shape and do not produce neurites, as can be seen in Fig. 3A. Following exposure to NGF, as shown in Fig. 3B, PC12 cells differentiate into neuronal type cells and begin to extend neurites into the periphery. The changes in morphology and cytoskeletal structure of cells exposed to varying levels of AMNPs were investigated at various timepoints using immunofluorescence for tubulin (fluorescein, green) and actin (TRITC, red) (Figs. 3C–E). The cells were fixed, permeabilized and stained with fluorescently labeled secondary antibody to primary anti-tubulin antibody-labeled microtubules, while actin microfilaments were labeled with fluorescent rhodamine phalloidin. Figs. 3C–E clearly indicate the dramatic reduction in PC12 cell ability to generate neurites following NGF induction with increasing concentrations of AMNPs. Fig. 3C shows immunofluorescent staining of typical control cells, with well-formed microtubules and actin microfilaments throughout the soma and neurites. Yet even with exposure to iron concentrations as low as 0.15 mM (Fig. 3D) there appears to be a reduction in the formation of actin microfilaments within the soma, as opposed to the normal appearance of the neurites, when compared to control cells. Furthermore, upon exposure to increasing AMNP concentrations, fewer microtubules extend to the periphery and the cells form less organized actin microfilaments within the main body, assuming an increasingly spheroidal shape, thus minimizing cell surface area and contact with the environment. This morphologic response to AMNPs continues to the point where, as in the case of 15 mM exposure (Fig. 3E), there appears to be little to no extended actin microfilaments within in the soma, the cells are spheroidal, exhibit minimal axonal/microtubule sprouting and fail to form mature neurites.

3.3. Diminished cellular response to a specific biochemical cue

While previous reports have also shown qualitative disruption of the cytoskeleton due to exposure to high concentrations of MNPs [13,21,22,24], this study investigates methods of quantifying phenotypic changes in cells as a function of exposure to increasing nanoparticle concentration. Normally, PC12 cells are characterized by their rapid and reversible response to NGF, resulting in the extension of neurite-like processes up to 1 cm in length, comparable to those of sympathetic neurons [29]. This profound and easily observable response makes PC12 cells an ideal model system for the study of neural stem cell development and differentiation, neurite regulation and outgrowth, and as a general model of cell response to biochemical cues. These changes can be readily quantified and, based on previous literature [32], the following parameters were used to compare the phenotypic response of cells exposed to AMNPs: frequency of neurite lengths, the number of neurites or "sprouts" extending from the soma, the number of branches per neurite, the number of intercellular processes and quantification of NGF-induced expression of specific proteins.

The most obvious effect that exposure to the AMNPs has upon the cells is their ability to generate mature neurites. The average number of neurites that sprouted from each [remaining] live cell (dead cells were not included) was measured at each of the three concentrations and compared with media only control (Fig. 4). Fig. 4A shows a typical NGF-stimulated PC12 cell in culture with arrows showing the location of its neurites (N) and a line delineating the length of an extended neurite. The data from these evaluations, plotted in Fig. 4B, shows the effect of AMNPs on the generation of neurites. Of the live cells evaluated, those exposed to 0.15, 1.5, and 15 mM AMNP iron concentrations on average produced 2.67, 1.9, and 0.97 neurites per cell ($n = 30$ cells/condition), respectively, as compared with 2.79 in the control cells. The lengths of the neurites which did extend were further evaluated, as shown in Fig. 4A. Of those cells that did sprout neurites (non-sprouting cells were not included), not only were there fewer neurites per cell, but also the lengths of the neurites that did extend were dramatically affected by exposure to AMNPs. In Fig. 4C, an inverse correlation between the level of AMNP exposure and the ability of the cells to respond normally to NGF and extend neurites into the periphery is seen. The histogram shows the frequency of neurite lengths of cells exposed to AMNPs at the tested concentrations. Notice the increasing inability of PC12 cells exposed to higher AMNP concentrations ($\geqslant$1.5 mM iron) to develop mature extended neurites, once again clearly indicating a negative relation between AMNP exposure and the production of neurites.

Similar to most neuronal type cells, the neurites of PC12 cells typically branch out in order to establish intercellular contacts. Such branching is vital to the formation of neuromuscular connections, synaptogenesis, neurite extension, regeneration and signal transduction associated with these processes. As such, formation of intercellular contacts is considered a metric of PC12 cell and neuronal morphology. Additionally, it has been readily established that disruption of these abilities results in diminished *in vivo* function and utility of neuronal type cells. Typical intercellular contacts (IC) for control cells (0 mM Fe) are shown in Fig. 5A. Fig. 5B shows that nanoparticle exposure reduces the ability of neurites to develop intercellular contacts and thus physically interact with one another. When plated at a standard density, the cells exposed to AMNPs fail to develop intercellular contacts at the same frequency as control cells. For each condition, the contacts (as indicated in Fig. 5A) of over 250 cells were

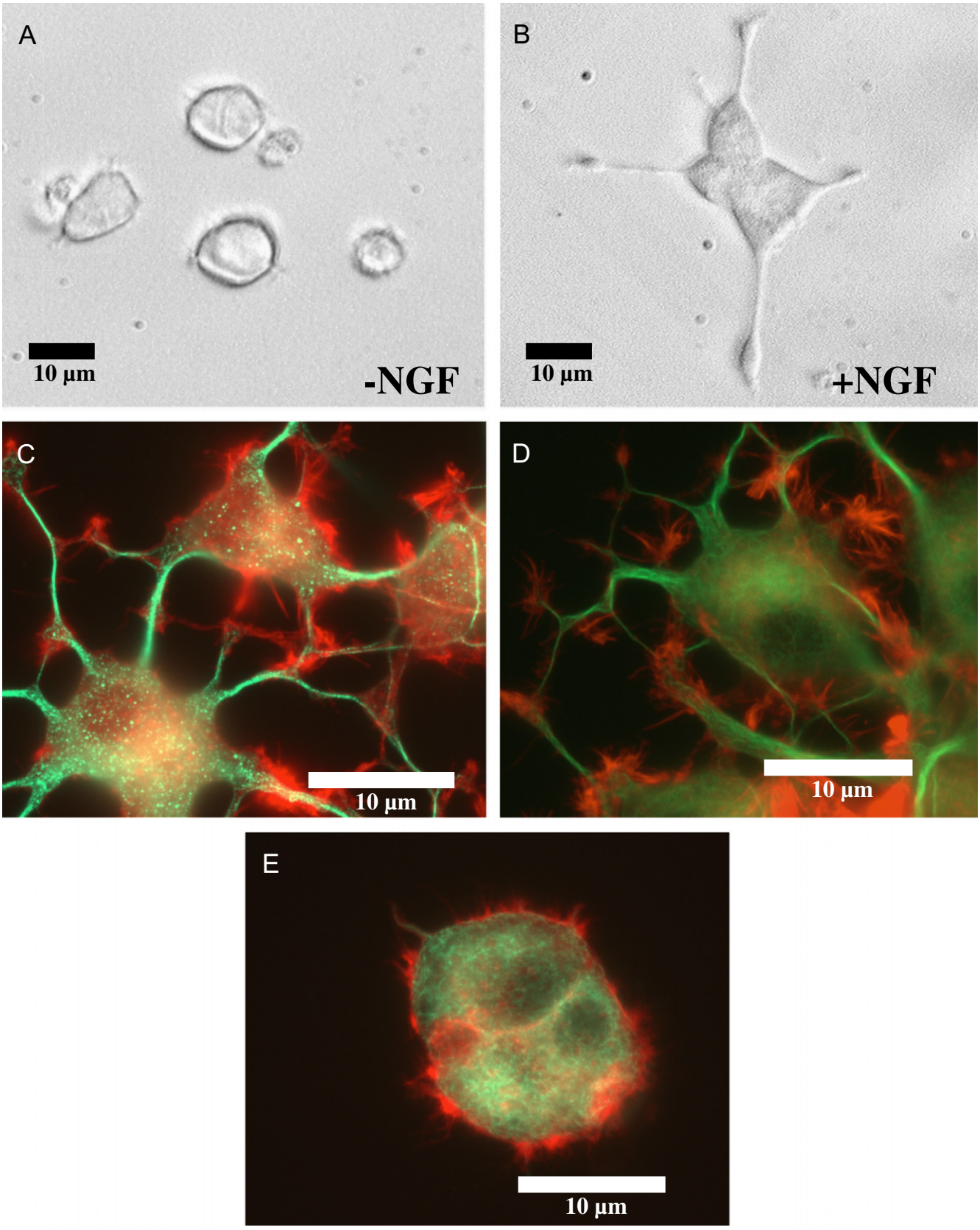

Fig. 3. Phase contrast images of PC12 cells, 48 h in culture (A) without NGF and (B) with NGF (+NGF). PC12 immunofluorescence for tubulin (green) and actin (red) at 6 days post AMNP exposure and 5 days post NGF exposure at Fe concentration of (C, control cells) 0 mM, (D) 0.15 mM and (E) 15 mM. Control cells form more actin microfilaments throughout the entire cell and produce more mature neurites than cells exposed to AMNPs.

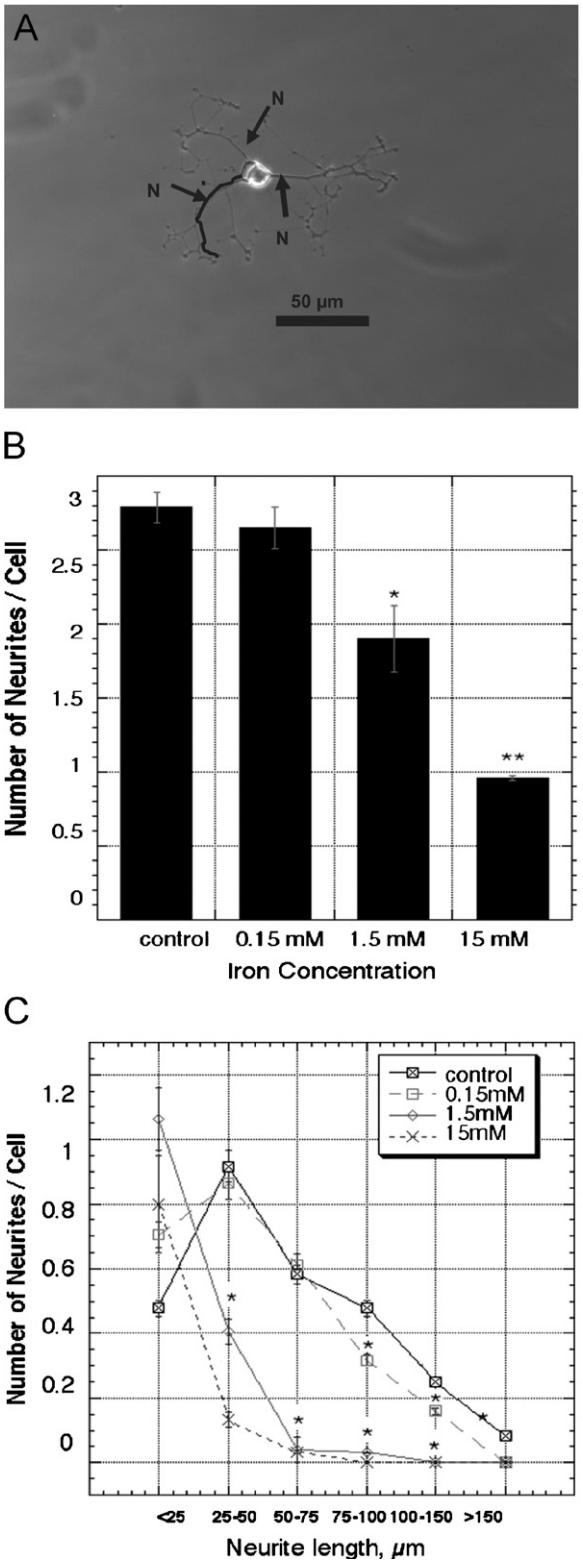

Fig. 4. Effect of AMNP exposure on neurite outgrowth of NGF induced PC12 cells at different Fe concentrations. (A) Phase-contrast micrograph of a typical PC12 cell showing a trace along the extension of the lower neurite (N) used for length calculation. Note reduced number of neurites (B and C), and reduced length of extended neurites (C) with increased AMNP Fe concentration 6 days post-exposure. (*Statistics*: ANOVA with Tukey's *post-hoc*, expressed as mean ± standard error, $*p<0.05$, $**p<0.01$.)

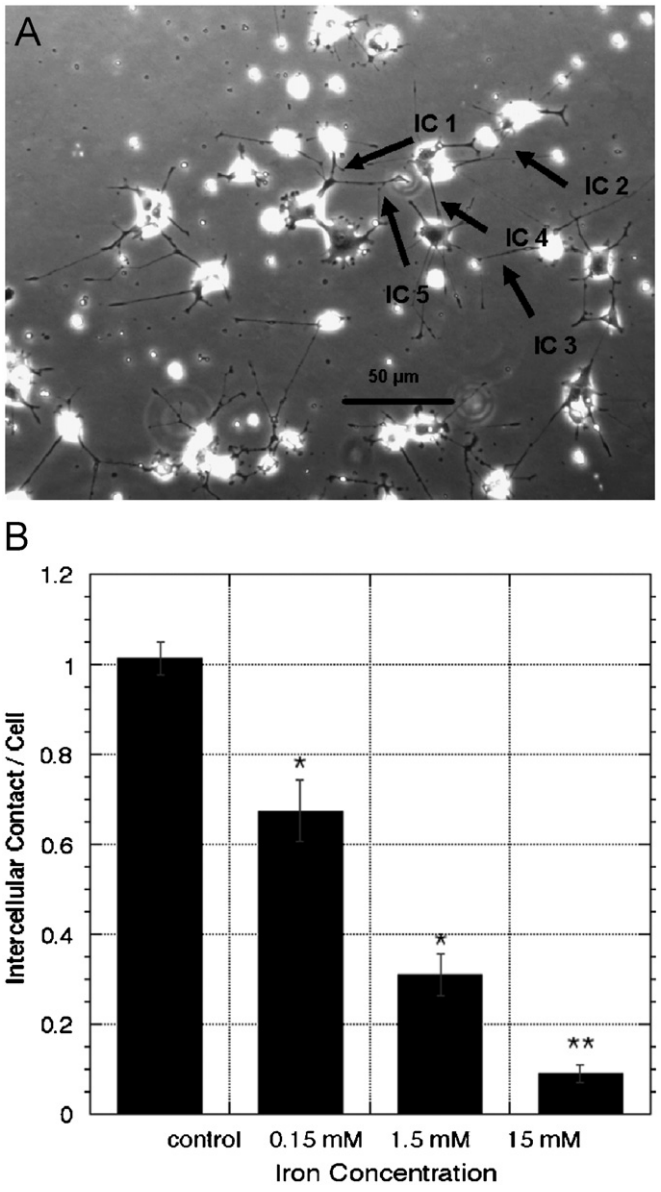

Fig. 5. Effect of AMNP exposure upon intercellular connections. (A) Phase-contrast micrograph of a typical NGF-induced PC12 cell showing intercellular contacts (IC) 6 days after AMNP exposure. (B) Number of intercellular contacts per cell versus AMNP Fe concentration 6 days post-exposure. (*Statistics*: ANOVA with Tukey's *post-hoc*, expressed as mean ± standard error, $*p<0.05$, $**p<0.01$.)

tallied and divided by the total number of cells. Even exposure to the most moderate of AMNP concentrations results in an over 30% reduction in intercellular contacts per cell (1.01 contacts/cell for control compared with 0.67 contacts/cell in 0.15 mM treated cells), likewise, higher concentrations further diminish intercellular communication (1.5 mM:0.31 contacts/cell; 15 mM:0.09 contacts/cell).

Lastly considered were the effects of AMNP exposure on the expression of protein related to axonal sprouting and neuronal function in order to determine whether the effects of exposure were strictly morphological or phenotypic as well. Growth-associated protein-43 (GAP-43) is a neuronal protein associated with axonal growth, neuronal plasticity

and learning and is necessary for the development and function of a variety of neuronal systems. GAP-43 has also been shown to be an efficient marker for the presence of neuronal growth cones [33]. Fig. 6(A) and (B) demonstrate a western blot of PC12 cell lysates using a monoclonal mouse anti-GAP-43 antibody, 6 days following exposure to various concentrations of AMNPs. HRP-tagged SDS-PAGE standards were used as molecular weight markers and β-actin blots were used as loading controls. Notice the decline in GAP-43 protein expression following exposure to increasing concentrations of AMNPs. Specifically, 0.15 mM AMNP iron concentration showed a GAP-43 band intensity comparable to the untreated control (C) and at [Fe] = 1.5 mM band intensity was significantly diminished, whereas GAP-43 levels were virtually undetectable in cells exposed to AMNPs at [Fe] = 15 mM.

Consistent with earlier literature [26], it was independently verified that DMSA concentrations (7.5, 75 and 750 μM) that are equivalent to or higher than the net concentrations of DMSA in experiments have little to no measurable effect on the parameters tested in these studies. While this certainly does not exclude the possibility that DMSA might have an effect upon these parameters when carried intracellularly into the cell, it does confirm that the effects seen here are not the result of DMSA exposure alone.

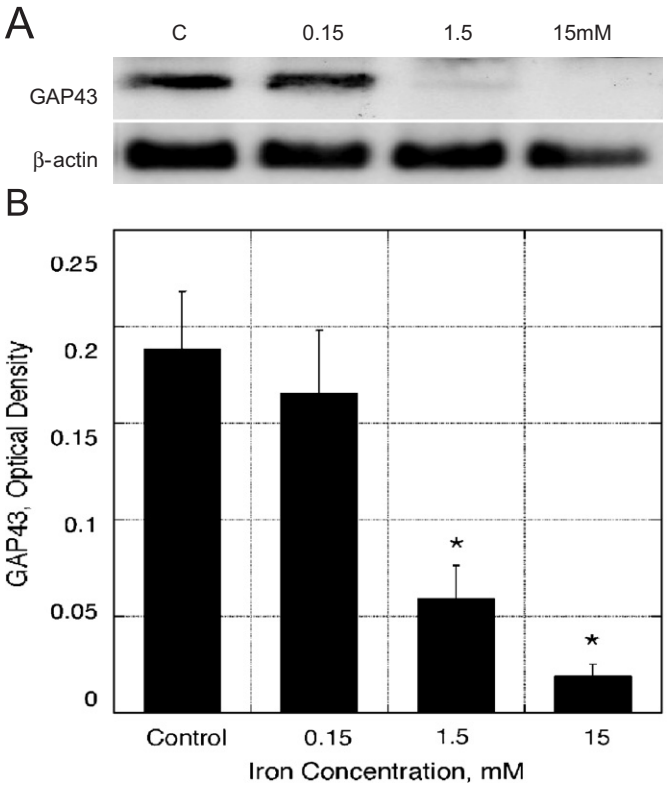

Fig. 6. (A) Western blot for growth associated protein, GAP-43 in NGF induced PC12 cells (normalized to β-actin, protein loading control) 6 days post AMNP exposure at [Fe] = 0 (C, control), 0.15, 1.5 and 15 mM. (B) Relative optical densities of GAP-43 bands shown in (A) ($n = 3$/group, $^*p < 0.05$.)

4. Discussion

This study indicates that even temporary exposure to Fe_2O_3 AMNPs results in a dose-dependent reduced ability of PC12 cells to appropriately respond to nerve growth factor. PC12 cells exposed to AMNPs show reduced viabilities, increased cytoskeletal disruption, and a diminished ability to form mature neurites in response to NGF exposure as compared to control cells. This may have significant implications for *in vivo* and phenotypic dependent *in vitro* uses of AMNPs and Fe_2O_3 MNPs in general. Overall, it was shown that the exposure of cells to even moderate concentrations of MNPs can adversely affect cell function, phenotype and viability. These findings also indicate and confirm previous reports that the presence of intracellular Fe_2O_3 nanoparticle constructs can result in significant changes in cell behavior and viability [21–23,34].

In light of these results and taking into account the results of other investigators, it seems that nanoparticle surface coatings, while perhaps innocuous themselves, can drastically affect the behavior of cells exposed to nanostructures coated with these agents. While the standard concentration of iron Fe^{3+} ions where cytotoxic effects normally begin to appear is roughly 4 mM [35], only the highest (15 mM) of the tested MNP concentrations exceeded this value, yet significant negative effects were seen at concentrations over 20-fold lower than the toxic level. It seems that there are three plausible explanations for this observation: first, that coordination of the coating agent with the nanostructure facilitates entry into or interaction with cells of both the nanostructure and surface chemicals, thereby magnifying any interactions (positive or negative) with cellular components; a second, alternative explanation is the variance in the effectiveness of the coatings to shield the nanostructures from [potentially adverse] interactions with cellular components; thirdly, there may also be a combination of these effects. The underlying causes of certain biological effects and interactions may be easier to diagnose than others, such as cytotoxic effects from known toxic nanostructures like cadmium selenide (CdSe)-based quantum dots, where toxicity differences between various coatings can almost certainly be explained through the second posited explanation [36].

In the present case, the observed cytotoxic effects are more difficult to diagnose, but are possibly due to free radical generation through Fenton and/or Haber-Weiss reactions whose effects only become noticeable at higher intracellular concentrations of iron [37]. Another possible explanation for the significant cytotoxicological, morphological and phenotypic effects of AMNP internalization is the apparent migration of the AMNP containing endosomes to the proximal perinuclear region of the PC12 cells, as shown in the TEM image in Fig. 1B, which may drastically impede transcriptional regulation and protein synthesis, such as GAP-43, resulting in loss of cell phenotype and possibly cell death. Yet the mere presence of intracellular Fe_2O_3 nanoparticles, even at the lowest

tested concentration, appears to affect cytoskeletal structure by either chemically or physically impeding actin microfilament formation in the main bodies of the cells and inhibiting the maturation and functions of neurites, such as the formation of intercellular contacts. In order to evaluate these possibilities, further studies into the physiochemical basis of the observed Fe_2O_3 cytotoxicity are necessary.

It should be noted that in the case of ferrofluid cytotoxicological studies, the implementation of a bare MNP control, while desirable, would raise more questions than it would answer. Firstly, an MNP coating is required for colloidal MNP stability in aqueous biological solutions making it unsuitable as an accurate comparison. Bare MNPs are highly unstable in saline solutions; form optically visible aggregates, and produce an interaction of such disparate physical characteristics so as to be irrelevant as a proper control against a stably dispersed ferrofluid. Furthermore, the effect of oxide nanoparticle solubility has recently been shown to directly affect the cytotoxicity of the material [35]. And lastly, the implementation of a different stabilizing coating would beg the question of which coating to utilize and what effect the other coating itself would have upon the cells.

5. Conclusions

In summary, this work has shown that exposure to increasing concentrations of anionic magnetic nanoparticles results in a dose-dependent diminishing ability of PC12 cells to differentiate in response to nerve growth factor. The results of our model system may act as a caveat for the use of AMNPs in neuronal experiments and in biomedicine in general. These results further imply that more study into the effects of cellular iron oxide internalization is both warranted and necessary and act to further bolster recent calls for increased attention and interest into the toxicity of nanomaterials [38,39]. Failure to fully and properly evaluate nanostructures on an individual case-by-case basis may lead to lack of parameter control in *in vitro* experiments, as well as incorrect assumptions concerning their biocompatibility and biosafety of their *in vivo* use.

Acknowledgments

We are sincerely grateful to Dr. Eduardo Macagno for his insightful conversations and general advice. We would also like to thank Chiara Daraio and Mariana Loya for all of their help and expertise in the TEM work. We additionally acknowledge the assistance of Norm Olson for TEM analysis using the UCSD Cryo-Electron Microscopy Facility supported by NIH Grants 1S10RR20016 and GM033050 to Dr. Timothy S. Baker and a gift from the Agouron Institute to UCSD. This work was supported by The University of California, San Diego and The American Society Engineering Education (ASEE), National Defense Science and Engineering Graduate (NDSEG) Fellowship.

References

[1] Ito A, Shinkai M, Honda H, Kobayashi T. Medical application of functionalized magnetic nanoparticles. J Biosci Bioeng 2005;100(1):1–11.
[2] Pankhurst QA, Connolly J, Jones SK, Dobson J. Applications of magnetic nanoparticles in biomedicine. J Phys D Appl Phys 2003;36(13):R167–81.
[3] Molday RS, Molday LL. Separation of cells labeled with immunospecific iron dextran microspheres using high-gradient magnetic chromatography. FEBS Lett 1984;170(2):232–8.
[4] Radbruch A, Mechtold B, Thiel A, Miltenyi S, Pfluger E. High-gradient magnetic cell sorting. Method Cell Biol 1994;42:387–403.
[5] Vasir JK, Labhasetwar V. Targeted drug delivery in cancer therapy. Technol Cancer Res T 2005;4(4):363–74.
[6] Scherer F, Anton M, Schillinger U, Henke J, Bergemann C, Kruger A, et al. Magnetofection: enhancing and targeting gene delivery by magnetic force in vitro and in vivo. Gene Ther 2002;9(2):102–9.
[7] Jordan A, Scholz R, Wust P, Schirra H, Schiestel T, Schmidt H, et al. Endocytosis of dextran and silan-coated magnetite nanoparticles and the effect of intracellular hyperthermia on human mammary carcinoma cells in vitro. J Magn Magn Mater 1999;194(1–3):185–96.
[8] Moroz P, Jones SK, Gray BN. Magnetically mediated hyperthermia: current status and future directions. Int J Hyperther 2002;18(4):267–84.
[9] Kircher MF, Allport JR, Zhao M, Josephson L, Lichtman AH, Weissleder R. Intracellular magnetic labeling with CLIO-Tat for efficient in vivo tracking of cytotoxic T cells by MR imaging. Radiology 2002;225:453.
[10] Lewin M, Carlesso N, Tung CH, Tang XW, Cory D, Scadden DT, et al. Tat peptide-derivatized magnetic nanoparticles allow in vivo tracking and recovery of progenitor cells. Nat Biotechnol 2000;18(4):410–4.
[11] Kohler N, Sun C, Wang J, Zhang M. Methotrexate-modified superparamagnetic nanoparticles and their intracellular uptake into human cancer cells. Langmuir 2005;21(19):8858–64.
[12] Sonvico F, Mornet S, Vasseur S, Dubernet C, Jaillard D, Degrouard J, et al. Folate-conjugated iron oxide nanoparticles for solid tumor targeting as potential specific magnetic hyperthermia mediators: synthesis, physicochemical characterization, and in vitro experiments. Bioconjug Chem 2005;16(5):1181–8.
[13] Gupta AK, Curtis AS. Surface modified superparamagnetic nanoparticles for drug delivery: interaction studies with human fibroblasts in culture. J Mater Sci Mater Med 2004;15(4):493–6.
[14] Zhang Y, Sun C, Kohler N, Zhang M. Self-assembled coatings on individual monodisperse magnetite nanoparticles for efficient intracellular uptake. Biomed Microdevices 2004;6(1):33–40.
[15] Bulte JW, Douglas T, Witwer B, Zhang SC, Strable E, Lewis BK, et al. Magnetodendrimers allow endosomal magnetic labeling and in vivo tracking of stem cells. Nat Biotechnol 2001;19(12):1141–7.
[16] Billotey C, Wilhelm C, Devaud M, Bacri JC, Bittoun J, Gazeau F. Cell internalization of anionic maghemite nanoparticles: quantitative effect on magnetic resonance imaging. Magn Reson Med 2003;49(4):646–54.
[17] Wilhelm C, Billotey C, Roger J, Pons JN, Bacri JC, Gazeau F. Intracellular uptake of anionic superparamagnetic nanoparticles as a function of their surface coating. Biomaterials 2003;24(6):1001–11.
[18] Wilhelm C, Gazeau F, Bacri JC. Magnetophoresis and ferromagnetic resonance of magnetically labeled cells. Eur Biophys J Biophy 2002;31(2):118–25.
[19] Kim JS, Yoon T-J, Yu KN, Kim BG, Park SJ, Kim HW, et al. Toxicity and tissue distribution of magnetic nanoparticles in mice. Toxicol Sci 2006;89(1):338–47.
[20] Lacava ZGM, Azevedo RB, Martins EV, Lacava LM, Freitas MLL, Garcia VAP, et al. Biological effects of magnetic fluids: toxicity studies. J Magn Magn Mater 1999;201(1-3):431–4.
[21] Berry CC, Wells S, Charles S, Aitchison G, Curds ASG. Cell response to dextran-derivatised iron oxide nanoparticles post internalisation. Biomaterials 2004;25(23):5405–13.

[22] Berry CC, Wells S, Charles S, Curtis ASG. Dextran and albumin derivatised iron oxide nanoparticles: influence on fibroblasts in vitro. Biomaterials 2003;24(25):4551–7.
[23] Hilger I, Fruhauf S, Linss W, Hiergeist R, Andra W, Hergt R, et al. Cytotoxicity of selected magnetic fluids on human adenocarcinoma cells. J Magn Magn Mater 2003;261(1–2):7–12.
[24] Zhang Y, Kohler N, Zhang M. Surface modification of superparamagnetic magnetite nanoparticles and their intracellular uptake. Biomaterials 2002;23(7):1553–61.
[25] Hussain SM, Hess KL, Gearhart JM, Geiss KT, Schlager JJ. In vitro toxicity of nanoparticles in BRL 3A rat liver cells. Toxicol In Vitro 2005;19(7):975–83.
[26] Aposhian HV, Aposhian MM. Meso-2,3-dimercaptosuccinic acid: chemical, pharmacological and toxicological properties of an orally effective metal chelating agent. Annu Rev Pharmacol Toxicol 1990;30:279–306.
[27] Wilhelm C, Gazeau F, Roger J, Pons JN, Bacri JC. Interaction of anionic superparamagnetic nanoparticles with cells: kinetic analyses of membrane adsorption and subsequent internalization. Langmuir 2002;18(21):8148–55.
[28] Greene LA, Tischler AS. Establishment of a noradrenergic clonal line of rat adrenal pheochromocytoma cells which respond to nerve growth factor. Proc Natl Acad Sci USA 1976;73(7):2424–8.
[29] Tischler AS, Greene LA. Nerve growth factor-induced process formation by cultured rat pheochromocytoma cells. Nature 1975;258(5533):341–2.
[30] Massart R, inventor; Agence Nationale de Valorisation de la Recherche (ANVAR), assignee. Magnetic fluids and process for obtaining them. US Patent No. 4329241, 1982.
[31] Fauconnier N, Pons JN, Roger J, Bee A. Thiolation of maghemite nanoparticles by dimercaptosuccinic acid. J Colloid Interf Sci 1997;194(2):427–33.
[32] Shubayev VI, Myers RR. Matrix metalloproteinase-9 promotes nerve growth factor-induced neurite elongation but not new sprout formation in vitro. J Neurosci Res 2004;77(2):229–39.
[33] Meiri KF, Pfenninger KH, Willard MB. Growth-associated protein, GAP-43, a polypeptide that is induced when neurons extend axons, is a component of growth cones and corresponds to pp46, a major polypeptide of a subcellular fraction enriched in growth cones. Proc Natl Acad Sci USA 1986;83(10):3537–41.
[34] Gupta AK, Gupta M. Cytotoxicity suppression and cellular uptake enhancement of surface modified magnetic nanoparticles. Biomaterials 2005;26(13):1565–73.
[35] Brunner TJ, Wick P, Manser P, Spohn P, Grass RN, Limbach LK, et al. In vitro cytotoxicity of oxide nanoparticles: comparison to asbestos, silica, and the effect of particle solubility. Environ Sci Technol 2006;40(14):4374–81.
[36] Hoshino A, Fujioka K, Oku T, Suga M, Sasaki YF, Ohta T, et al. Physicochemical properties and cellular toxicity of nanocrystal quantum dots depend on their surface modification. Nano Lett 2004;4(11):2163–9.
[37] Symons M, Gutteridge J. Free radicals and iron: chemistry, biology and medicine. Oxford: Oxford University Press; 1998.
[38] Nel A, Xia T, Madler L, Li N. Toxic potential of materials at the nanolevel. Science 2006;311(5761):622–7.
[39] Service RF. Nanotechnology. Calls rise for more research on toxicology of nanomaterials. Science 2005;310(5754):1609.